A&A 411, L215–L222 (2003)
DOI: 10.1051/0004-6361:20031436

Astronomy & Astrophysics

Cosmic rays tracks on the PICsIT detector⋆

A. Segreto[1], C. Labanti[2], A. Bazzano[3], A. J. Bird[4], E. Celesti[2], and M. Marisaldi[2,5]

[1] IASF/CNR, sezione di Palermo, via Ugo la Malfa 153, 90146 Palermo Italy
[2] IASF/CNR, sezione di Bologna, via P. Gobetti 101, 40129 Bologna Italy
[3] IASF/ CNR sezione di Roma, via del Fosso del Cavaliere 100, 00133 Roma, Italy
[4] School of Physics and Astronomy, University of Southampton, Highfield, Southampton SO17 1BJ, UK
[5] Dipartimento di Fisica Universita' di Bologna, Viale B. Pichat 6/2, 40127 Bologna

Received 15 July 2003 / Accepted 16 September 2003

Abstract. Since the first in orbit activation of the PICsIT detector, frequent spikes have been noticed in its count rate. Tracks in the detector images, corresponding to the spikes, indicate that these events are generated by interaction of cosmic rays with the detector plane.
Since these events constitute a significant fraction of the instrument background, a dedicated study has been performed and it has been clarified that the mechanism that leads to spikes and track formation is related to the presence in the CsI crystals of phosphorescence states having decay times of the order of 100 ms. We have also shown that these events, thanks to their temporal characteristics, can be removed from the PICsIT data when the instrument is in Photon by Photon mode.
Moreover, thanks to the pixellated structure of the PICsIT detector, we have also obtained evidence of the presence of numerous electromagnetic and hadronic showers generated by the primary cosmic rays.

Key words. PICsIT – CsI – cosmic ray – electromagnetic showers – hadronic showers

1. Introduction

PICsIT is one of the major subsystems of the IBIS telescope on board INTGRAL (Ubertini et al. 2003), and is an imaging detector layer consisting of an array of 64×64 pixels.

A PICsIT pixel is made of a 3 cm long CsI(Tl) scintillator bar with a square cross-section of 8.4×8.4 mm^2 wrapped with a thin layer of white reflective paper and optically glued to a custom-made silicon PIN photodiode (Labanti et al. 2003).

Each PICsIT pixel has its own readout electronics so that they can be considered as independent detection units. The 4096 pixels are arranged in 8 independent modules, each containing an array of 16×32 pixels.

2. The cosmic ray spikes

Soon after the in-orbit activation of PICsIT, the presence of frequent spikes in the detector count rate became evident (Fig. 1); such spikes were only observed on a very few occasions during the ground calibrations.

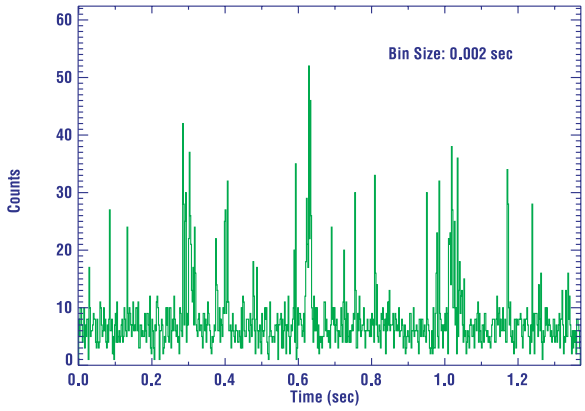

Fig. 1. A typical in-orbit count rate of the PICsIT detector. It is evident the presence of many spikes per second.

The presence of tracks of bright pixels in detector images (Fig. 2) is a clear indication that the spikes are due to the interaction of cosmic rays with the detector. However it is to be noted that the response of the pixels to the cosmic rays is considerably different from the response to γ rays.

In fact, when a typical γ ray photon interacts with a CsI crystal, the scintillation light generated is converted, by the pixel electronics, to one single event. On the contrary, after the interaction with a cosmic ray, the pixel starts to generate a sequence of events. It is this multiplicative effect that is

Send offprint requests to: A. Segreto,
e-mail: segreto@pa.iasf.cnr.it

⋆ Based on observations with INTEGRAL, an ESA project with instruments and science data center funded by ESA member states (especially the PI countries: Denmark, France, Germany, Italy, Switzerland, Spain), Czech Republic and Poland, and with participation of Russia and USA.

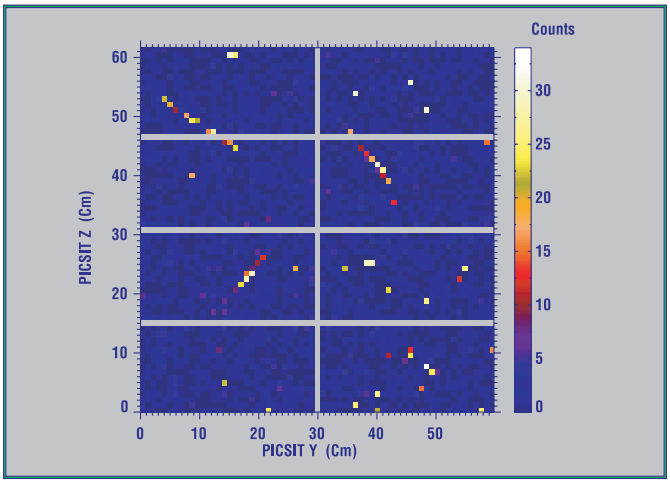

Fig. 2. Image of the PICsIT detector plane integrated in 1.4 s. Note as in some pixels there are more than 30 counts while on average there are only few counts per pixels. Tracks produced by cosmic rays are evident.

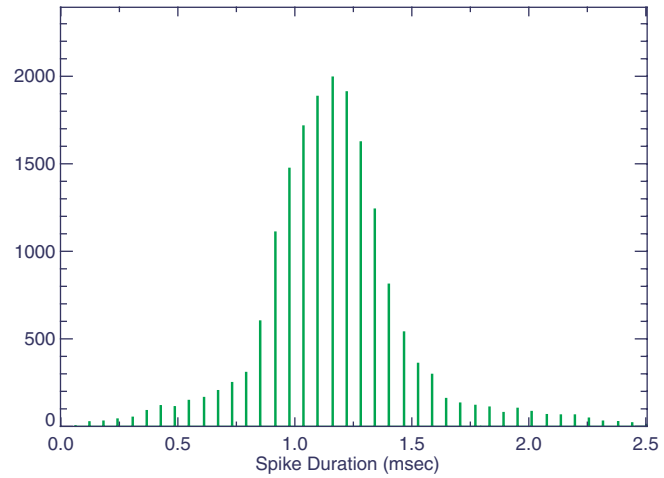

Fig. 3. Distribution of the spike duration. The gaps in the distribution are due to the limited time resolution of the instrument.

responsible for the spike formation and that makes the pixels that have generated these events clearly visible in the detector images.

Thanks to their peculiar timing characteristics, an algorithm for the extraction of the events induced by cosmic rays can be implemented. In fact, a group of events on the same pixel can be considered as generated by a cosmic ray when the time separation between any event and the previous one is less than a certain time threshold.

Since the average time separation between successive events in a spike is about 100 μs, a 1 ms time threshold is enough to identify nearly all the spikes, reducing at the same time the possibility of chance coincidences to very low values.

The distribution of the spike duration is shown in Fig. 3; it is evident that the average duration of a spike is 1.2 ms, with 0.3 ms standard deviation. The distribution of the number of events per spike is shown in Fig. 4.

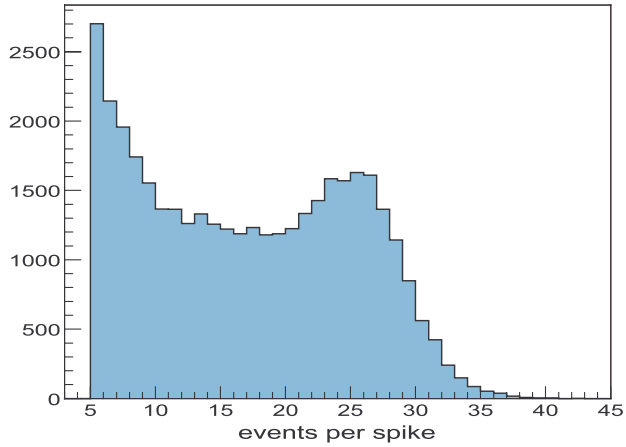

Fig. 4. Distribution of the number of events per spike. Only spikes with more than 4 events are considered.

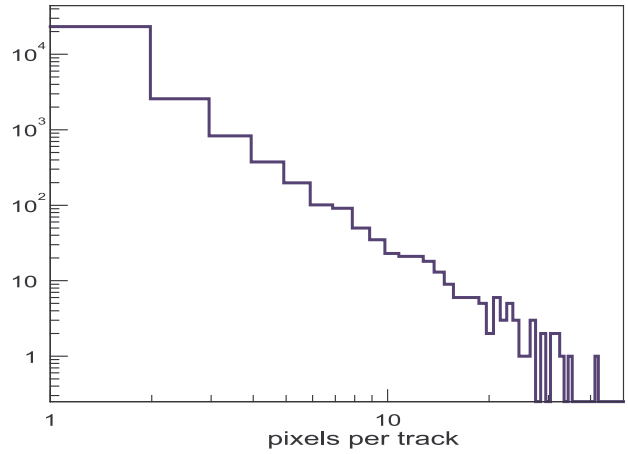

Fig. 5. Distribution of the number of pixel per spike. Only pixel generating spikes with more than 4 events have been selected. The total live time of the data set considered is about 2260 s.

3. Cosmic ray tracks

Depending on the arrival direction, a single cosmic ray may interact with many pixels at the same time, leaving a track of bright pixels in the detector image.

An algorithm for track detection has been implemented which is able to recognize sets of pixels that generate spikes having temporal and spatial correlation, and to merge them into a single track.

A pixel is associated to a track if the time separation between its spike and the track is less than a maximum time limit (chosen to be 10 ms), and the spatial distance between the pixel and the track is less than a maximum distance limit (chosen to be 4.2 in pixel units).

In a data set of about 2260 s we have found about 38 000 spikes with more than 4 events which have been rearranged in about 27 700 tracks; the resulting distribution of the number of pixel per track is shown in Fig. 5.

Most of the spikes are associated with an isolated pixel and only in 6.6% of the cases are there tracks made of more than 2 pixels; only 0.6% of the tracks is made of more than 9 pixels.

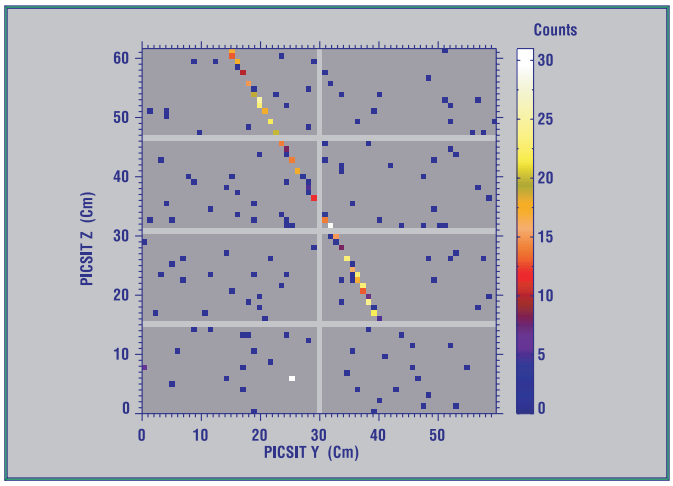

Fig. 6. A long straight track one pixel wide. This track is clearly originated, through direct ionization loss, by a single charged particle.

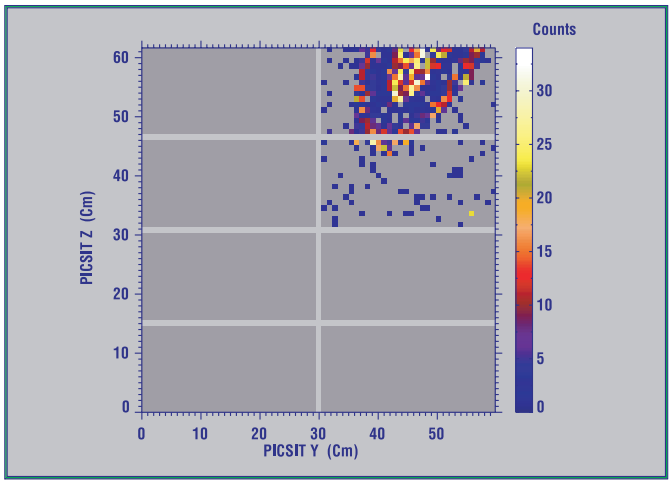

Fig. 7. An almost perfect elliptical track. Only a conical shower of secondary particles illuminating the detector plane can originate this kind of shape.

Reasonable variations of the parameters (maximum time and distance limit) in the track reconstruction software do not change this situation very much.

4. Cosmic ray induced showers

Tracks of bright pixels, one single pixel wide, like in Fig. 6, are clearly generated, through direct ionization loss, by a single charged particle travelling in the detector plane. However in the detector images we also found, sometimes, tracks constituted by sets of bright pixels filling quite extended areas. In some cases these areas have an elliptical shape like the one shown in Fig. 7.

The only possible explanation for the observed phenomenon is that the PICsIT detector layer has been illuminated by a shower of secondary particles originating above (or below) the detector layer, caused by the interaction of a primary cosmic ray with the structure of the satellite, as shown in Fig. 8.

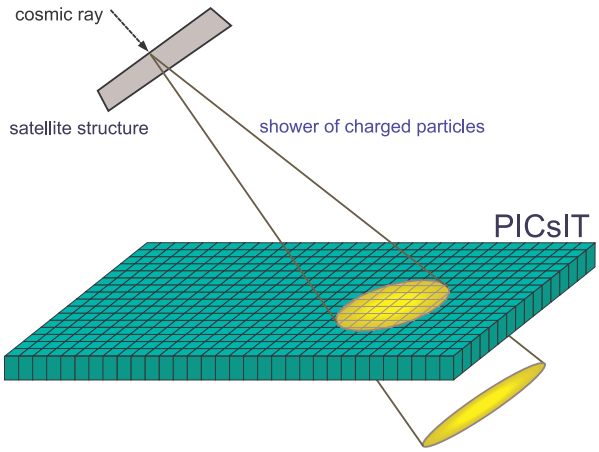

Fig. 8. A cosmic ray, interacting with the satellite structure, can originate a shower of secondary particles that illuminate extended areas of the detector plane. Depending on the kind of incident cosmic ray the shower can be electromagnetic (initiated by γ, e^+, e^-) or hadronic.

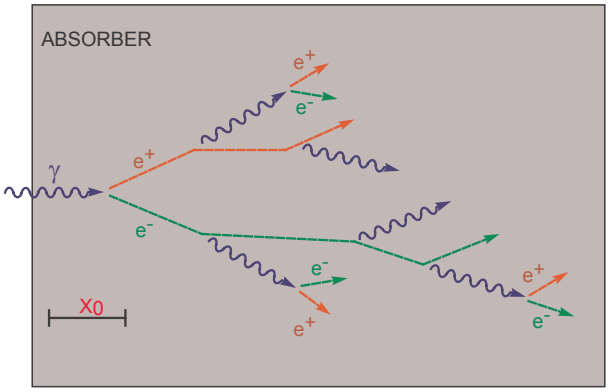

Fig. 9. The electromagnetic shower originates when an high-energy photon (or e^- or e^+) is incident on an absorber. If the energy is sufficiently high, it starts a multiplicative cascade of secondary electrons and photons via bremsstrahlung and pair production. As the shower develops it broadens laterally due to multiple scattering. X_0 represent the radiation length of the material.

Two physical processes that can be at the origin of showers of charged particles are the Electromagnetic and the Hadronic cascade.

The Electromagnetic shower (Fig. 9) is generated by high-energy photons and electrons (or positrons) which, passing through matter, start a multiplicative cascade of secondary electrons and photons via bremsstrahlung and pair production. The shower expands spatially during propagation due to the multiple scattering.

The Hadronic showers are instead initiated by high-energy particles (neutrons, protons, pions, etc.) that, interacting with the nuclei of atoms via strong nuclear forces, transform part of their energy into new hadrons, mostly pions, initiating a multiplicative process. In a "Hadronic shower" the penetrating core, containing mainly pions, continually produces electromagnetic sub showers through the $\pi^0 \rightarrow \gamma\gamma$ decay.

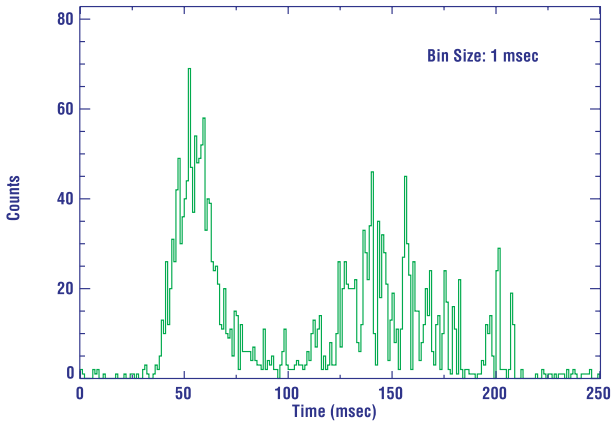

Fig. 10. The pulse correspondent to the elliptically shaped track. The total length of this pulse is 170 ms and it is composed by 2500 counts. It is formed by the superposition of many spikes (~1.2 ms each) having a temporal modulation in the average number of events per spike.

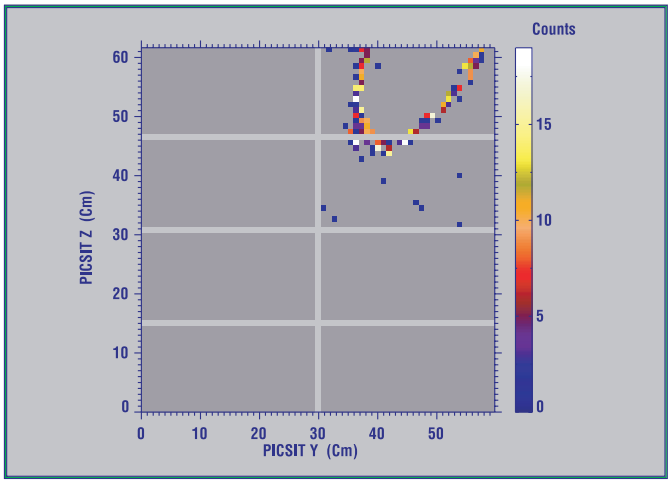

Fig. 11. The image obtained selecting only the events in the first 20 ms of the pulse. It is clear that the pixels on the perimeter are the first to generate spikes.

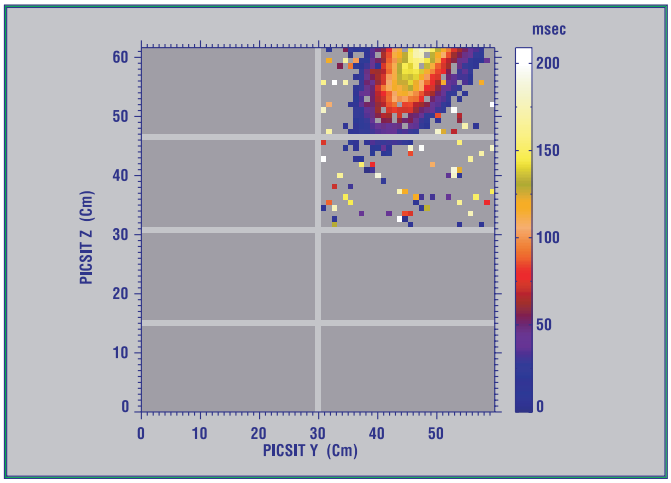

Fig. 12. This image has been obtained representing, for each pixel, the delay (in ms) of the events generated by each pixel after the common shower start time. The pattern observed can be related to the natural radial variation of the particle density in the shower illuminating the detector plane.

4.1. Temporal and spatial analysis of a shower track

When a shower illuminates extended areas of the detector, huge pulses, with thousands of counts given the numerous pixels involved, are generated. These pulses have a quite long time duration, up to hundreds of ms, and a complex temporal profile (Fig. 10).

Temporal analysis at pixel level reveals that each illuminated pixel contributes to the collective pulse only with a single spike having the same 1.2 ms average duration as the spikes generated by the interaction of the pixel with a single primary cosmic ray.

The quite long duration of the collective pulse is then exclusively due to the fact that there can be a significant delay from the time when the pixels are excited (which is essentially the same for all the illuminated pixels) and the time at which the pixels generate their own spike.

The average number of events per spike, probably for some effect generated by the pixel electronics, is a function of time, thus originating an intensity modulation in the total pulse.

It can be also easily shown that the pixels illuminated by a shower do not generate spikes at a random time after the initial excitation, but that the delay of the spikes depends on the relative position of the pixel inside the area.

This fact is shown in the image in Fig. 11 which has been obtained integrating the first 20 ms of the pulse. It is clear that only pixels in the external perimeter of the illuminated area contribute to the first part of the pulse.

The correlation between the pixel position and the spike delay in a track generated by a shower, can be better visualized in a detector image where, for each pixel, the intensity represents the delay of the first event after a common start time.

The delay map so obtained (Fig. 12) shows very clearly how the spike generation starts from the pixels on the perimeter and then proceeds toward the centre, following concentric ellipses.

The extreme spatial coherence in the image, and the pattern observed is a clear indication that the spike delay must be related to some physical variable in the shower of secondary particles having a radial variation.

4.2. The CsI phosphorescence

The presence of phosphorescence states has been already considered by Hurley (1978) in order to explain pulses several hundred milliseconds long observed in CsI crystals exposed to primary cosmic ray radiation.

Also in our case, the long delay observed between the pixel excitation and the spike generation can be related to the presence of these phosphorescence states. The sequence of events, illustrated in Fig. 13, is then:

– when the charged particles interact with the CsI crystals, a great number of long lived phosphorescence states are excited;

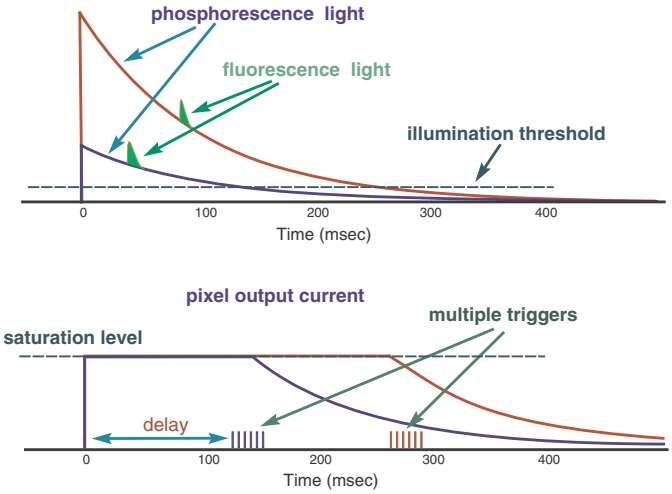

Fig. 13. The upper figure shows the CsI crystal light evolution for two different initial level of excitation. Below is represented the correspondent pixel output current. Only after a delay dependent on the initial excitation, the pixel electronics starts to generate a set of triggers. No other trigger can be generated during this delay (N.B. the decay time are arbitrary)

- the level of phosphorescence light emitted by the CsI crystals is so high that the pixel output current reaches a saturation level, and remains stable, at a constant value, for a quite long time after the initial excitation;
- when the phosphorescence light reduces under some critical threshold the pixel output current start to decrease from its saturated value. Only at this time, probably because of ripples, a set of numerous events are generated by the pixel electronics.

Note that during the delay between the initial excitation and the spike generation, the pixels cannot generate any other event. In fact, the additional scintillation light generated by the absorption of a real photon in the crystal cannot produce any increase in the already strongly saturated pixel output current.

Assuming that the number of phosphorescence photons after the initial excitation (N_0) decay exponentially with a natural time constant τ_{ph}, their time evolution, $N_{ph}(t)$, is given by

$$N_{ph}(t) = N_0 * \exp(-t/\tau_{ph}). \quad (1)$$

If N_c is the illumination level below which the pixel output current exits from saturation, we deduce that the spikes are generated after a delay (δ) given by

$$\delta = \tau_{ph} * \log(N_0/N_c). \quad (2)$$

The process outlined above explains the correlation between the pixel position and the spike delay observed in the shower tracks.

In fact, apart from small variations in the physical parameters of the pixels (τ_{ph}, N_c), the spike delay depends, essentially, only on the number of the initially excited phosphorescence states, that is, from the amount of energy deposited in each CsI crystal.

The delay map then represents, on an approximately logarithmic scale, the spatial distribution of the energy deposited by the shower in the detector and the pattern observed is generated by the natural radial decrease of the particle density from the shower axis.

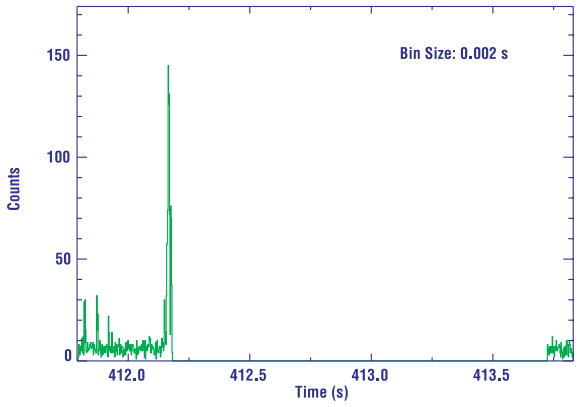

Fig. 14. A gap in the PICsIT count rate generated by the detection of an extended shower. Only the first part of the shower pulse is transmitted on-ground.

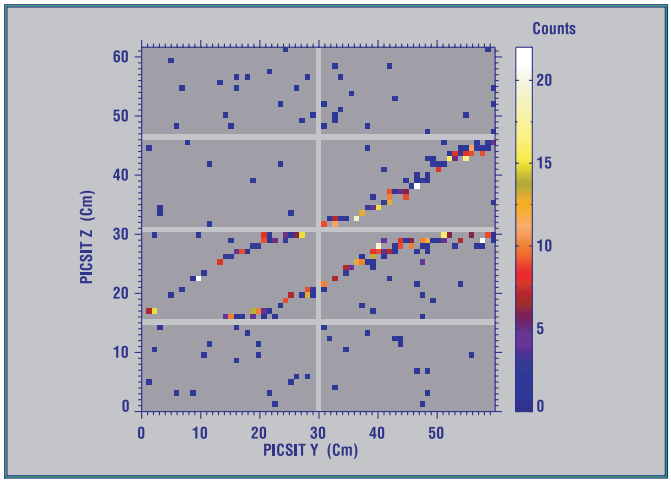

Fig. 15. A largely incomplete shower track. By the few events transmitted on-ground, it is anyway possible to deduce that the total area illuminated by the shower was ~450 cm^2, which is one of the most extended.

4.3. Telemetry loss

Due to the high number of pixels involved in an extended shower, the counts generated are often too many to be transmitted on ground, given the limited IBIS telemetry.

So, in most cases, it happens that the events generated by the pixels in the perimeter of the illuminated area, which are the first to generate spikes, are enough to fill the telemetry buffers. This fact generates a gap in the PICsIT count rate a few ms after the start time of the pulse (Fig. 14).

As a consequence of this loss of telemetry, most of the images of extended showers are largely incomplete (Fig. 15) or resemble closed loop tracks like the one in Fig. 16. Note the lack of any background event in the region internal to a closed loop track; this is the direct consequence of the fact that the pixels in the internal region, during the considered time

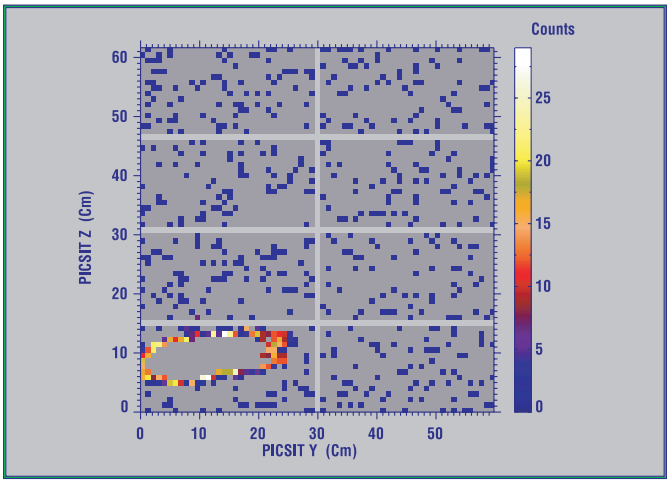

Fig. 16. Image of a partially transmitted shower track. The fact that there are no background events inside the closed loop, confirm that all the pixels in the internal region are in a saturated state.

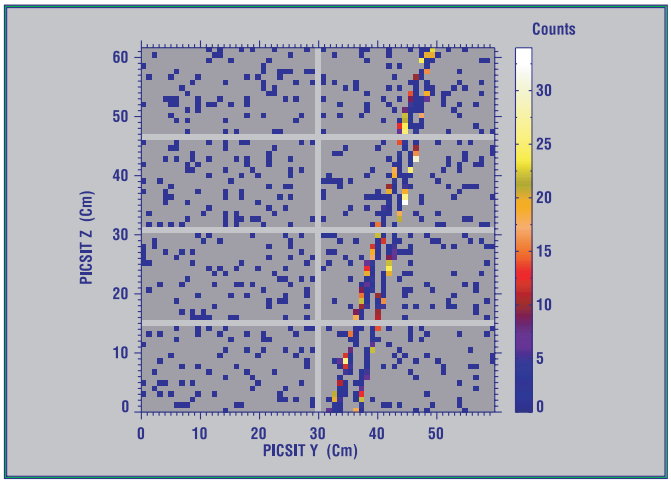

Fig. 17. This track is in too long to be of pure electromagnetic origins so it should be an hadron shower. Due to a telemetry gap only the pixel in the shower border are present.

interval, are in a saturated state, during which they cannot generate any signal.

4.4. Shower topology

The tracks having an elliptical shape are clearly generated by conical showers illuminating the PICsIT detector plane from outside. In some cases, however, the shape of the track indicates that the shower originates from inside one of the CsI crystals.

In these cases, when the arrival direction of the cosmic ray is parallel to the detector plane, we can actually get an image of the whole spatial development of the shower and, from the track extension it is sometimes possible to discriminate whether its origin is purely electromagnetic or hadronic.

The longitudinal development of a purely electromagnetic shower (which can be initiated only by γ, e^+ or e^-) is characterized by the radiation length (X_0) of the material, and its lateral extension, which is determined by multiple scattering, by the Moliere radius (R_M) (Barnett 1996).

A material thickness corresponding to ~20 radiation lengths is enough to contain more than 99% of the electromagnetic shower and most of its energy is deposited within few Moliere radii around the shower axis.

In contrast to this, the longitudinal development of hadron showers is governed by the nuclear interaction length (λ_I) and, by transverse momenta of secondary particles as far as lateral width is concerned.

For CsI the radiation length is $X_0 = 1.85$ cm and its Moliere radius is $R_M = 3.8$ cm while the nuclear interaction length is $\lambda_I = 36.5$ cm; hadron showers are thus longer and wider than electromagnetic shower.

Figure 17 shows an example of a track that, given its longitudinal extension, is almost certainly due to an hadronic shower.

An image gallery of the delay maps for some of the showers detected by PICsIT is shown in Fig. 18. The shower pulse duration, always of the order of few hundredths of ms, is an indication of the huge amount of energy deposited by a cosmic ray through this process.

5. Energy spectrum and data cleaning

Due to the mechanism of spike generation, the total number of background events induced by the cosmic rays is much higher than the number of incident particles.

Moreover, the generation of these events is distributed in a time interval (on average of 1.2 ms) which is much longer than the anticoincidence time window, so they are essentially unaffected by the IBIS VETO system.

Figure 19 shows a comparison between the PICsIT total background spectrum and the spectrum of the events generated by cosmic rays. It is clear that they are responsible for ~10% of the total PICsIT background and for up to ~30% of the background in the lowest energy range.

Given their peculiar temporal characteristic this background component can however be completely removed from the data when the instrument is in photon-by-photon mode, as shown in Fig. 20. Of course, this cannot be done when the energy spectra are integrated on-board since, in that case, we have no timing information.

6. Conclusions

We have analyzed the spikes visible in the PICsIT count rate and found they are related to the presence of long lived phosphorescence states in the CsI crystal excited by the passage of cosmic rays.

These events, being delayed with respect to the cosmic ray arrival time, constitute a background component not reduced by the IBIS VETO system but that can be removed when the instrument is in photon by photon mode.

Beside tracks associated with the passage of a single, ionized particle, we have found tracks generated by showers illuminating extended areas of the detector plane and shown that it

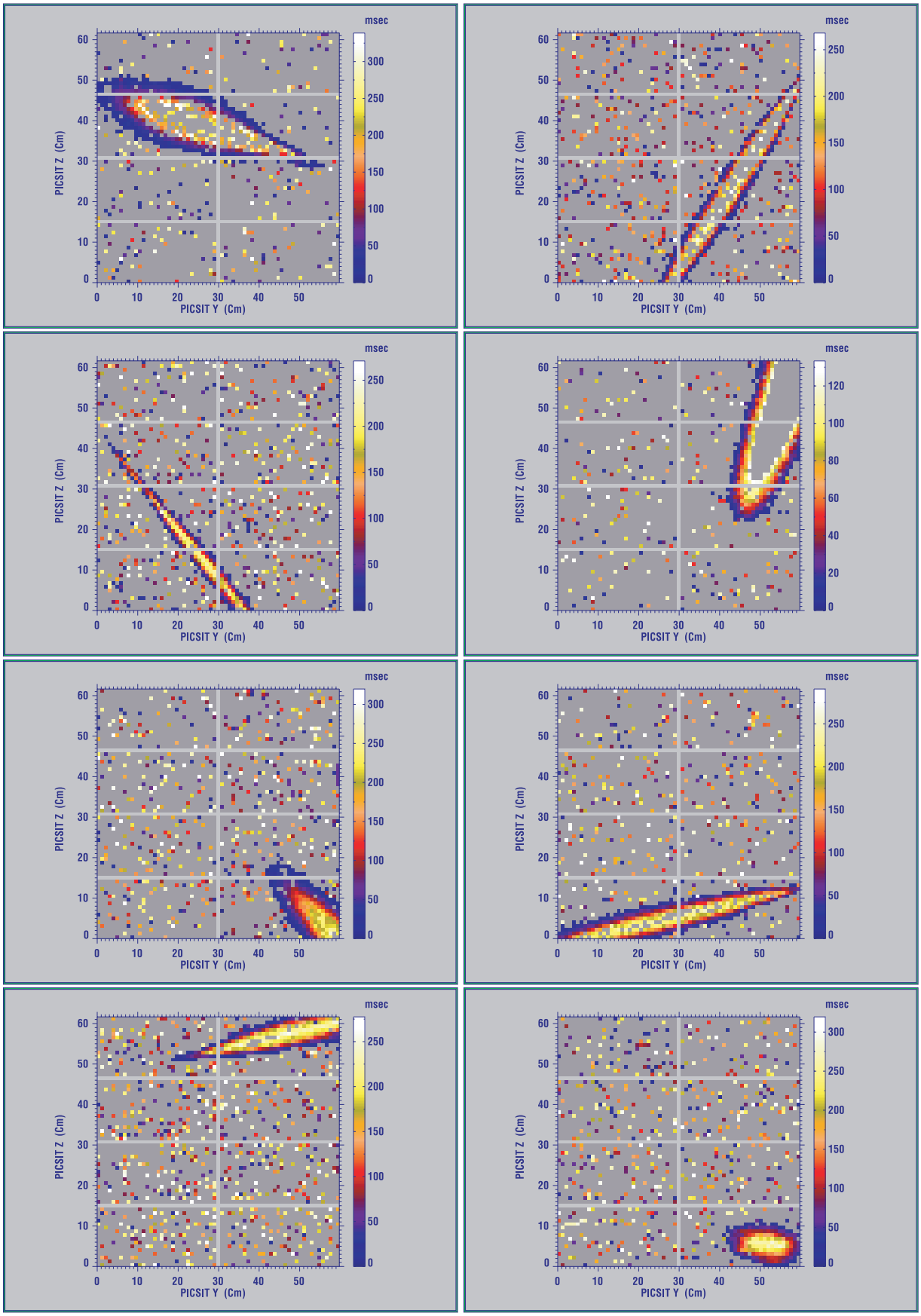

Fig. 18. Image gallery of shower tracks: the color scale represents the time delay of the first event generated by each pixel with respect to the beginning of the shower pulse. For the pixels illuminated by the shower, the delay depends on the energy deposit. Many tracks are incomplete due to telemetry gaps.

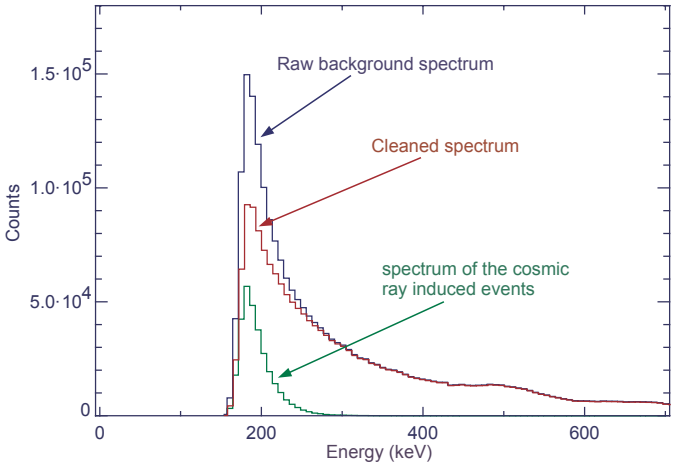

Fig. 19. The total PICsIT background spectrum compared with the spectrum of the events induced by cosmic rays. In the low energy channels, up to 30% of the background counts are due to this unexpected component.

is possible to generate images representing the spatial development of these showers.

This unexpected characteristic could be useful for testing simulation codes of shower development in CsI calorimeters like the ones that will be used in the next high-energy experiment (GLAST, AGILE). Moreover, it should be seriously considered that, depending of the size of the CsI crystals used, a permanent phosphorescence background could severely degrade their performance.

Since we have evidence that huge energy deposits in PICsIT detector are associated with extended showers, we can deduce that the same kind of phenomenon is possibly at the origin of the strong spikes observed in many other detectors using inorganic scintillators (e.g. BeppoSAX GRBM, PDS, OSSE) and generally believed to be due to ionization loss by high Z cosmic rays. Through shower generation, charged or uncharged particles may indeed release a very high fraction of their energy in these kind of detectors.

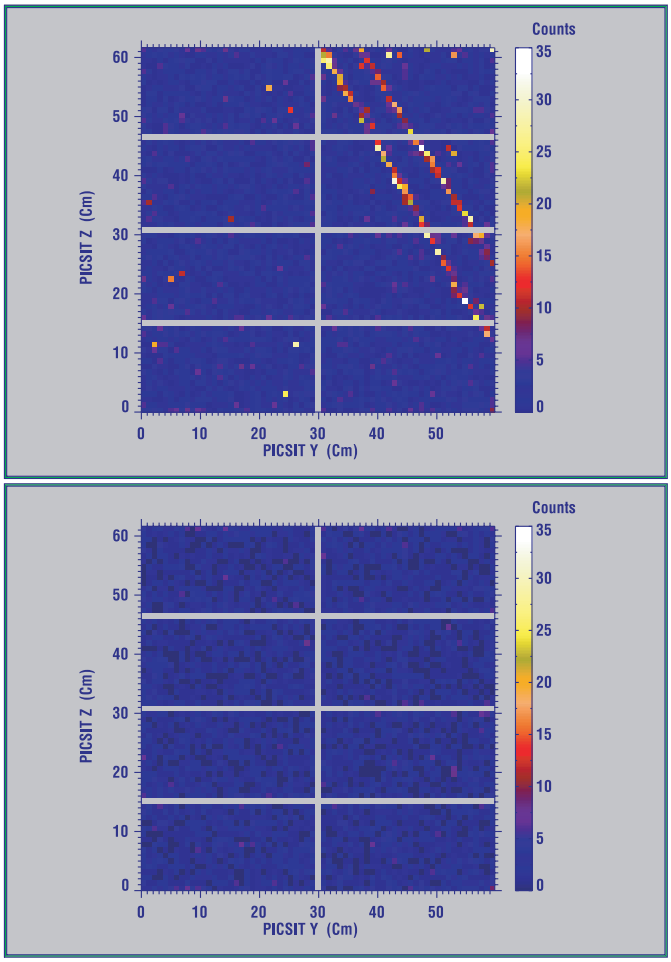

Fig. 20. A PICsIT detector image before and after the cleaning from the events generated by cosmic rays.

References

Barnett, R. M., Carone, C. D., Groomet, D. E, et al. 1996, Phys. Rev. D54, 1

Hurley, K. 1978, A&A, 69, 313

Labanti, C., Di Cocco, G., Ferro, G., et al. 2003, A&A, 411, L149

Ubertini, P., Lebrun, F., Di Cocco, G., et al. 2003, A&A, 411, L131